Step-wise Overlay Technique for the Mapping of Unconfined Groundwater Potential Zone in Tectonically Controlled Landforms

Ihsan, H, M.,[1] Hadi, M, P.[2] and Sartohadi, J.[3]
[1]Graduate School of Universitas Gadjah Mada, Indonesia
[2]Faculty of Geography, Universitas Gadjah Mada, Indonesia
[3]Faculty of Agriculture, Universitas Gadjah Mada, Indonesia

Abstract
The existence of unconfined groundwater in tectonically-controlled volcanic landforms is continuous and discontinuous as in alluvial landforms. DEM-NAS is a product available all over Indonesia and has the potential for unconfined groundwater mapping. The study was conducted by applying GIS techniques to obtain information on drainage density, TWI (Topographic Wetness Index), slope angle, and lineament density with openly available algorithms. All parameters are put on the map using fuzzy analysis techniques before being combined using a step-wise overlay technique. Classification of unconfined groundwater potential was done based on the value of the merging parameter map. The results of the field verification show that 44 springs are in the potential zone with an area percentage of 68.01%, and 10 springs are in the less potential zone with an area percentage of 31.99%.

1. Introduction

The existence of unconfined groundwater in tectonically-controlled volcanic landforms is continuous and discontiouos as in alluvial landforms. Medium to low groundwater potential is usually found in weathered and cracked hard rocky areas with high elevation and very steep topography, while flood plain zones are usually associated with good groundwater potential due to high infiltration levels of alluvium sediment (Thapa et al., 2017). Volcanic landforms have high elevation and steep topography. The tectonical activity in volcanic landforms causes hard material to slowly weathered. The existence of groundwater storage is usually in volcanoes associated with sediment, especially pumice (Singh et al., 2019). The existence of groundwater is affected by geomorphological units such as plains, terraces, volcanoes, hills, valleys and material conditions (Sandoval and Tiburan, 2019).

The study of groundwater can be identified by hydrological, geological, geophysical, and remote sensing approaches (Venkateswaran and Ayyandurai, 2015). Exploration of groundwater through hydrogeological, geological and geophysical techniques requires a great deal of cost and time (Jha et al., 2010, Razandi et al., 2015 and Murmu et al., 2019). Remote sensing and GIS (Geographic Information System) are efficient tools in mapping groundwater potential by reducing time and energy (Nithya et al., 2019). DEM (Digital Elevation Model) is a product that can be processed into parameters for the existence of potential groundwater with the help of spatial technology (Elbeih, 2015). DEM can obtain terrain aspects such as drainage density, slope angle, lineament density (Al-Shabeeb et al., 2018) and TWI (Topographic Wetnes Index) (Setiawan et al., 2019).

The study of groundwater potential using the step-wise overlay approach (tiered overlapping analysis) has never been done in a tectonically-controlled area. The mapping method of groundwater potential is usually performed by several methods, such as: the MCDA (Multi-Criteria Decision Analysis) method carried out in *Guna tana* area in the upper blue Nile Basin, Ethiopia (Andualem and Demeke, 2019), the hybrid computational intelligence model carried out in Vadora District, Gujarat, India (Pham et al., 2019), GA (Genetic Algorithm) method performed in Wuqi Country, Shaanxi Province, China, and comparisons of groundwater potential methods between AHP (Analytic Hierarchy Process), Catastrophe and entrophy techniques in Trichinopoly, India (Jenifer and Jha, 2017). The whole method is carried out by utilizing remote sensing technology and GIS.

The objective of this study was to apply the step-wise overlay technique in the tectonically-controlled landforms in Garut Basin, West Java

Province, Indonesia for mapping the unconfined groundwater potential. The landforms studied are in the form of hilly zones surrounded by young volcanoes so that the spatial distribution patterns are distinctly different. Tectonical activity is characterized by the existence of faults, touches, synclines and anticlines in the study area. The study parameters used were drainage density, TWI, slope angle, and lineament density. The DEM used is DEM-NAS, available for data studies throughout Indonesia. This study is expected to be useful for the effective and efficient study of groundwater potential in similar landforms.

2. Study Area

The area of tectonically-controlled landforms is in the northwestern part of the Garut Basin with an area of 229.54 km². Garut Basin is located in Garut Regency, West Java Province, Indonesia. The Garut Basin is surrounded by a volcanic cone morphology. These conditions cause the Garut Basin to have a varied topography, slope angle, and elevation, from flat to mountainous. The basic materials of this area are andesite and basalt. Based on the Garut-Pamempeuk regional geological map, there are faults, synclines, anticlines and geologic contact, so this area is a tectonically-controlled volcano quarter (Figure 2).

The study area is divided into 3 areas (Table 1), namely structure 1, structure 2 and structure 3 (Figure 1). Structure 1 is the landform dominated by highlands but there is a rain shadow area with an area of 129 km². Structure 2 is the landform dominated by lowlands, this area is adjacent to the landforms of volcanic plains with an area of 57.66 km ². Structure 3 is the landform dominated by semi-highlands but it is not exist rain shadow area with an area of 42.78 km².

3. Data and Method

The study of groundwater potential using DEM data produced by BIG (Geospatial Geoinformation Agency) is accessed on http://tides.big.go.id-/DEMNAS/Jawa.php and available for all areas in Indonesia. BIG stated that the DEM is called DEM-NAS which has a spatial resolution of 0.27 arcsecond. DEM-NAS is used to generate groundwater parameters such as river flow density, TWI (Topographic Wetness Index), slope angle, and lineament density.Data developed for zoning analysis of groundwater potential are morphology, lithology and hydrology (Setiawan et al., 2019).

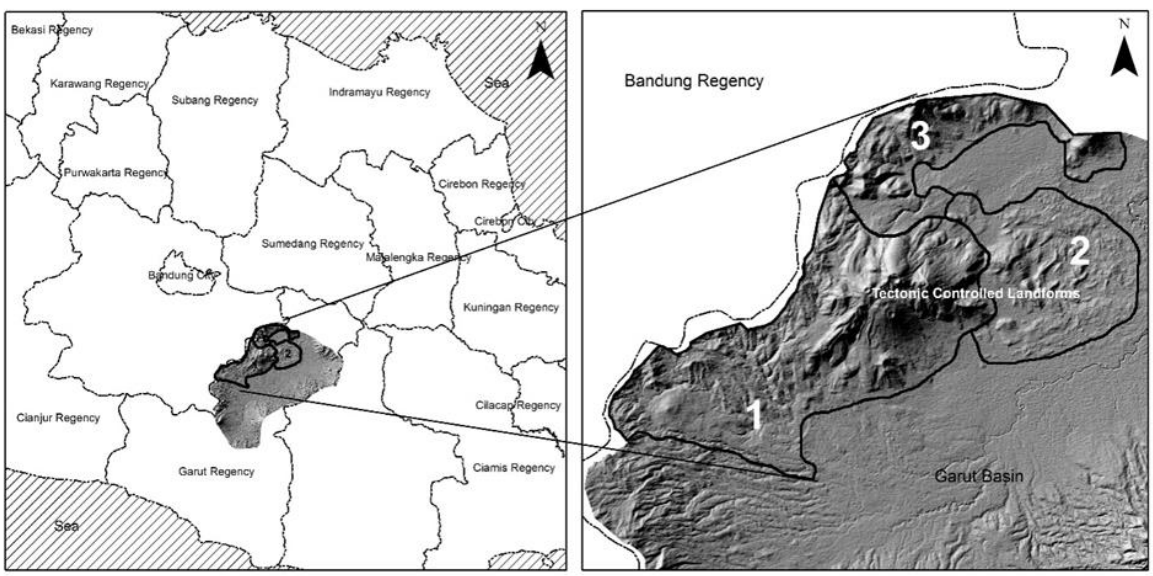


Figure 1: Study site of tectonically-controlled landforms

Table 1: Characteristics of the study area

Location	Elevation	Morphology	Relief	Existing
Structure 1	2238-746	Structural fault with a lava dome	Dominated by Mountainous area (>40°)	Rain Shadow Area
Sturcture 2	1648-596	Structural faults with parasitic cones	Dominated by Hilly area (15°-40°)	Not a Shadow Area
Structure 3	1062-613	Structural faults with Alluvial	Dominated by Wavy area (8°-15°)	Not a Shadow Area

DEM is able to generate hydrogeological data such as drainage density, slope angle (Das, 2019), TWI (Topographic Wetness Index) (Misi et al., 2018), and lineament density (Wilson and Gallant, 2000).

3.1Drainage Density

Drainage density is the total length divided by the total area in each river flow (Horton, 1932). The closeness of the channel and the nature of the surface material can be shown through the river flow density in km/km² (Venkateswaran and Ayyandurai, 2015). Areas with high river flow density values cause infiltration power to decrease and runoff to rise, so the groundwater potential is at a low value of river flow density (Al-adamatand Al-shabeeb, 2017). DEM is able to extract river flow data with the direction algorithm method on the plugin arc hydro tool (Yousif et al., 2018). The results of river flow extraction will produce several river orders. The flow used is an order which is a perennial not periodic river. Drainage density can be calculated based on the following Horton formula (1932):

$$\mathrm{d} = \sum_{i=1}^{n} Di/A(km^2)$$

Equation 1

The formula explains that d is the river density index (km/km²), *Di* is the length of the river including its tributaries (km²) and A is the area. River flow density can be analyzed using ArcGis software with the plugin arc hydro tools and lineament density (Oikonomidis et al., 2015).

3.2 TWI (Topographic Wetness Index)

The TWI study funtions to measure topographic control in the hydrological process (Setiawan et al., 2019). TWI is able to describe the spatial pattern of water-saturated areas, which is the key to understanding the diversity of materials and hydrological processes (Grabs et al., 2009). The higher the TWI value, the lower the slope angle value. and the more the groundwater potential (Nejad et al., 2017). The physical properties of the soil and parent material have a correlation to the TWI calculation results (Gillin et al., 2015). TWI calculationis carried out based on formulas made by Beven and Kirby (1979):

$$\mathrm{TWI} = \mathrm{In}\left(\frac{\alpha}{\tan\beta}\right)$$

Equation 2

The formula explains that α is the area of the unslope contributing area and β is the slope angle. Variable α (m²) and β (m) are performed based on DEM extraction using SAGA GIS 2.3.2 software. DEM is able to be used to develop TWI analysis (Sorensen and Sorensen, 2007).

3.3 Slope Angle

Slope angle is one of the parameters that has a role in recharge control of groundwater potential. Groundwater potential is usually at a low slope angle value (Hammouri and Al-amoush, 2014). Steep slope angles produce small absorption, because water flows in the direction of gravity according to its degree, so it does not have adequate time to infiltrate the surface and replenish the saturation zone (Yeh et al., 2016). The slope angle is the main indicator of groundwater infiltration below the surface, usually on flat slopes and slow surface runoff, causing a lot of time for rain water to infiltrate and high infiltration power (Murasingh et al., 2018). The slope angle can be generated through DEM data by extracting processed GIS software slope (Patra et al., 2018). The characteristics of the slope angle are described through the classification of Van Zuidam (1985) to clarify the description of the slope angle class in the study area.

3.4 Lineament Density

In the remote sensing description, lineament is often reflected as ridge line and valleys with the traditional method of line extraction, which is based on artificial visual or semi-automatic interpretations (Han et al., 2018). The lineament in this study is a straight-shaped feature associated with the valley, because the groundwater potential is in a flat area. The greater the value of lineament density or the closer it is to large faults, the higher the permeability (Al-Rozouq et al., 2019). GIS technology is able to identify the lines by utilizing DEM data (Rajasekhar et al., 2018). Lineament density can be calculated using the following formula:

$$d = \frac{\sum_{i=1}^{i=n} Li}{A}$$

Equation 3

Where LD is the lineament density$\sum_{i=1}^{i=n} Li$, is the total length of the lineament (L), and A is the area of landforms. High Ld value indicates the high porosity and groundwater potential (Yeh et al., 2016). The lines can be analyzed using PCI Geomatica software. The lineament density is mapped using ArcGIS Software by utilizing the density function tools (Al-adamat and Al-shabeeb, 2017).

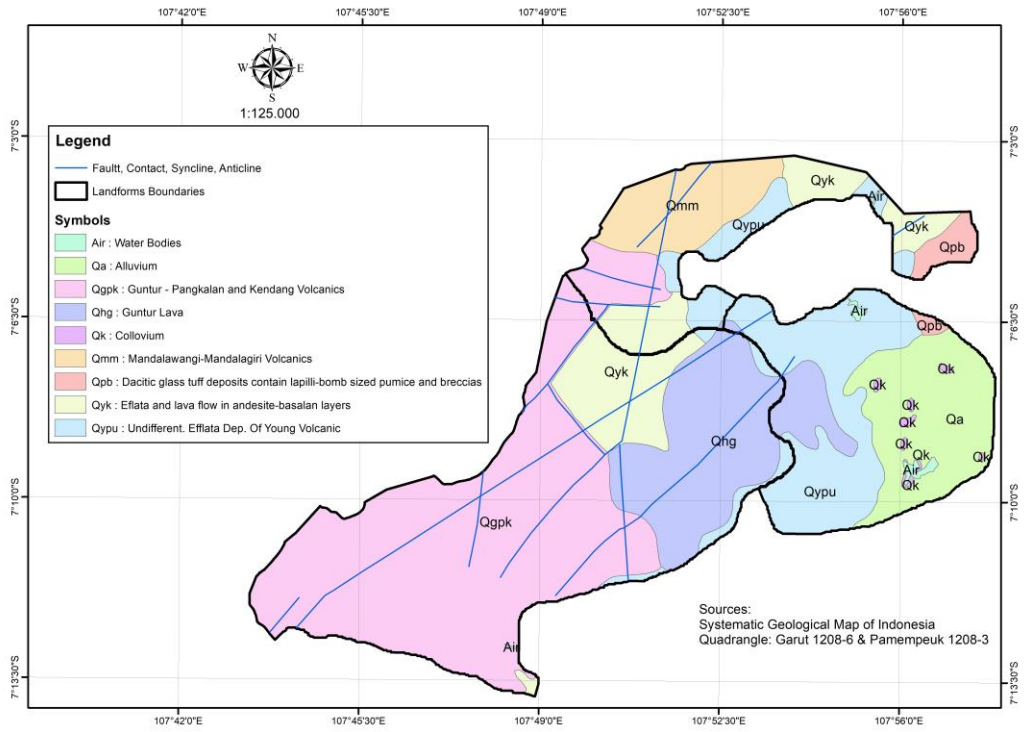


Figure 2: Geology map of study area

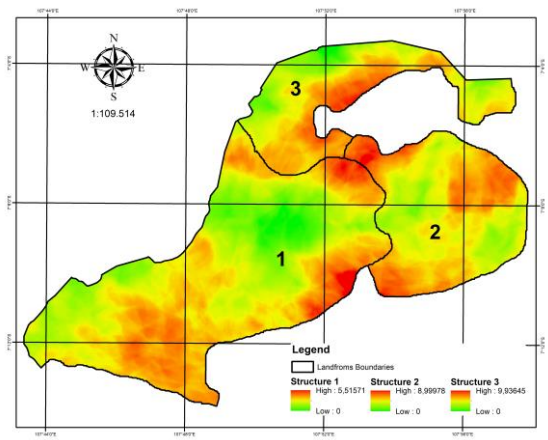


Figure 3: Drainage density

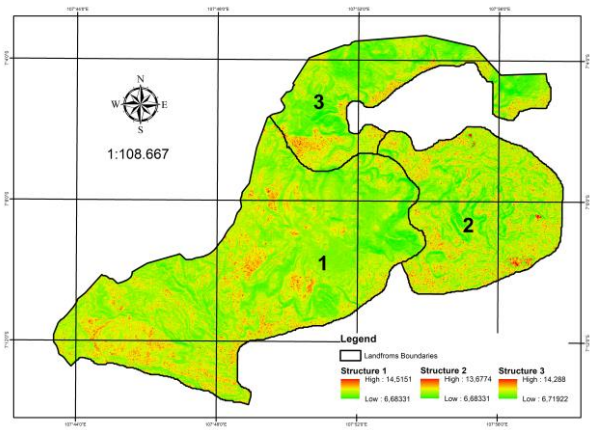


Figure 4: Topographic wetness index

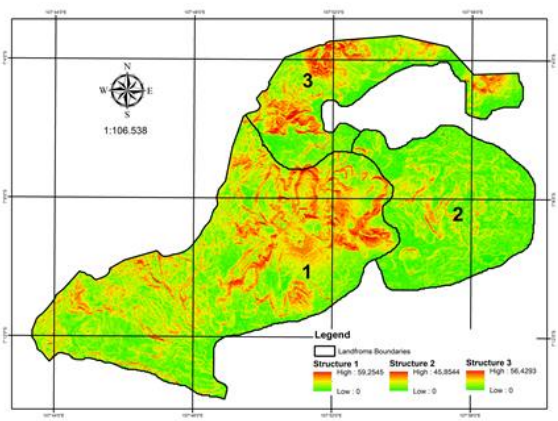


Figure 5: Slope angle

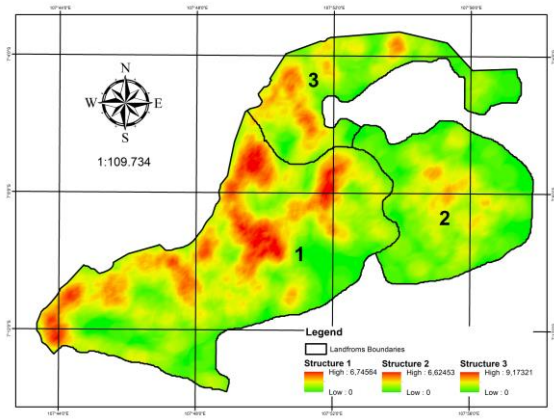


Figure 6: Lineament Density

3.5 Zoning of Groundwater Potential

The method used for zoning groundwater potential is stepwise overlay. This method is basically an overlay, but it is done in stages from one to four parameters (Table 2). The overlay method in GIS induces complex matrix changes, produces binary changes in the image without changing the major minor landscape, and is based on classification (Tiede, 2014). Each tiered parameter overlay will show different results, but the more parameters, the better the accuracy assumed.

Table 2: Step-wise overlay of groundwater Parameters

No	Landforms	Study Paramaters
1	Structure 1	Drainage density (2) + TWI (1)
	Structure 2	
	Structure 3	
2	Structure 1	(Drainage density + TWI) (2) + Slope (1)
	Structure 2	
	Structure 3	
3	Structure 1	(Drainage density + TWI + Slope) (2) + Lineament density (1)
	Structure 2	
	Structure 3	

The processing results of each parameter of unconfined groundwater (Drainage Density, TWI, slope angle and lineament density) were raster data that will be processed through fuzzy membership to equalize raster values with a range of value 0-1 in ArcGis software. Parameter weights were determined by trying to overlay each parameter in rotation until finding a good value (Table 2).

Zoning verification of groundwater potential was done by surveying the location of a spring, then the coordinates location was plotted. The sampling technique used was purposive sampling because the existence of groundwater was unknown in number and location, so the numbers were determined based on field conditions. Zoning classification of groundwater potential was divided into two, namely potential area and less potential area. The step-wise overlay method was applied to each area of structure 1, structure 2 and structure 3.

4.1 Drainage Density

Analysis of river flow using hydro arc tools shows that the shape of structure 1 and structure 3 has 7 river orders while structure 2 has 6 river orders. In each form, the river order 1 and 2 are not used, because it is assumed that the river is perennial. The level of infiltration in the area around the perennial river is greater than in the intermittent river. Groundwater potential is at a low drainage density level, due to low infiltration rates (Al-adamat and Al-shabeeb, 2017). The length of the river structure 1 for order 7-3 is 242.64 km, structure 2 for order 7-3 is 112.98 km and structure 3 for order 6-3 is 88.64 km. The total area determines the length of the river in tectonically-controlled landforms. The wider the area, the longer the river flows.

Drainage density in tectonically-controlled landforms has a great value located in highlands, but springs are rarely found in structure 3 with a density value of 0 - 9.94 km². The structure 3 is has the lowest area and length of river, compared to other structures. The tectonical activity causes differences in the length and density of river flows, because the material in this area is brittle and it forms streams and river flows. The structure 1 has a river flow density value of 0 - 5.56 km², while the structure 2 is 0 - 8.99 km². Presentation of drainage density in spatial form illustrates the high and low of an area, so that the distribution of groundwater potential will appear based on parameters of drainage density (Figure 3)

4.2 TWI (Topographic Wetness Index)

The TWI study on tectonically-controlled landforms has a value with a small difference, even almost the same between structure 1, structure 2 and structure 3. In tectonically-controlled landforms, the TWI value of structure 1 is 6.74-14.51, structure 2 is 6.68 - 13.68 and structure 3 is 6.72 - 14.29. This condition is caused by the formation process of the same land and material originating from volcanoes. Based on the geological map of the Pamempeuk-Garut sheet from the Geological Agency, typical volcanic rocks such as andesite-basalt, breccias and tuffs are found.

Surface material is produced from extrusive volcanoes that surround the Garut Basin. The striking difference in TWI value depends on relief units such as upper volcanic slope, middle volcanic slope, lower volcanic slope, caldera, old volcanic hills, old volcanic plains, old volcanic mountains, valley floor, collovial slopes and subresent lava flows (Figure 4).

High TWI value is found in areas with flat topography. A high TWI value is assumed to have a high infiltration rate, due to the existence of non-steep terrain, allowing small runoff. The TWI study functions to measure topographic control in the hydrological process (Setiawan et al., 2019). TWI is able to describe the diversity of materials and hydrological processes through the spatial pattern of water-saturated areas (Grabs et al., 2009). Based on a 1: 50,000 semi-detailed soil map from BBLSDP (Center for Agricultural Research and Development on Land Resources), haplic andosol, district cambisol, haplic podzolic, rodic latosol and gleisol district were found. The soil unit in the study area

has good drainage and smooth texture.

4.3 Slope Angle

In general, the slope angle in the tectonically-controlled landforms is dominated by hilly to mountain relief classes (16°-35°). Classification of slope angles from hilly to mountainous (16°-35°) in structure 1 has an area of 60.89 km² and structure 3 has an area of 17.03 km². Based on the Van Zuidam slope angle classification (1985) the area of structure 1 and structure 3 has 7 classifications, such as flat to almost flat (0°-2°), wavy (2°-4°), wavy to corrugated (4°-8°), corrugated to hilly (8°-16°), hilly to mountainous (16°-35°), steep mountains (35°-55°) and very steep mountains (>55°). The structure 2 has 6 slope angle classifications.

The classification of very steep mountain slope angle (> 55°) is not found in the structure area 2. This condition is due to the fact that structure 2 is dominated by corrugated to hilly slope angle classes (8°-16°) with an area of 18.12 km². The structure 2 is adjacent to the volcanic landforms. The condition of the slope angle has groundwater potential because it has a longer residence time for rainwater and a high infiltration rate (Patra et al., 2018). The highest slope angle is in the structure 1 which is 59.25 ° (Figure 5).

4.4 Lineament Density

The study of lineament applied PCI Geomatic software shows straight-shaped features on the surface of the earth. This lineament is valley and ridge. In this study, the lineament used is valley because the groundwater potential is in a flat area such as valleys. The extraction results were manually sorted using ArcGIS based on the hillshade and color appearance of the DEM-NAS. A low DEM-NAS value indicates low elevation or valley, while a high DEM-NAS value is the ridge. Based on the analysis, 650 lineaments are found in structure 1 with a length of 301.28 km, 161 lineaments are found in structure 2 with a length of 67.76 km, and 170 lineaments are found in structure 3 with a length of 75.85 km. The number of lineaments is affected by terrain conditions which are undulating terrain and total area.

The lineament is rarely found in flat areas, due to less varied topographic conditions such as those in the structure 2. The lineament can be an indication of the existence of structure in an area. The existence of structures must be further verified based on field data and geological maps. Based on the geological map of the Pamempeuk-Garut sheet from the Geological Agency, the tectonically-controlled landform has a structure of faults, anticline, syncline and geologic contact. The lineament density is determined by the number of lineaments and the area. Based on the analysis, structure 1 has a lineament density of 0-6.75 km², structure 2 has a lineament density of 0-6.62 km², and structure 3 has a lineament density of 0 - 9.17 km². Areas with high lineament values are areas with high groundwater potential, due to high permeability (Al-Rozouq et al., 2019). The distribution of lineaments density is depicted through raster data which is an infographic of the existence of groundwater potential (Figure 6).

4.5 Unconfined Groundwater Potentials

DEM-NAS is able to analyze the study of groundwater potential using parameters of drainage density, TWI (Topographic Wetness Index), slope angle and lineament density. Based on field verification there are 54 springs in tectonically-controlled landforms (Figure 7). Step wise overlay analysis shows 44 springs in potential landforms with an area of 156 km² (68.01%) and 10 springs in areas with less potential landforms with an area of 73.42 km² (31.99%) (Table 3).

The stepwise overlay method shows that everytime each parameter is added, the number of springs in a potential landform increases or remain the same as the number of springs in potential landforms, while the total area increases or decreases.The results of the step wise overlay analysis on stage 1 analysis (drainage density + TWI) has the same number of springs as stage 2 analysis (drainage density + TWI + slope angle), which is 41 springs in potential landforms and 13 springs in less potential landforms (Table 2). This condition is because TWI and slope angles both have topographic control functions of rainwater runoff and infiltration.

Stage 3 analysis is the result of step wise overlay for all parameters. Structure 1 has the highest number of springs in the potential landform. This area is dominated by highlands and includes mountainous areas. In the western part of the structure 1 there is a rain shadow area. Groundwater sources are indicated to originate from orographic rain that occurs in mountains and tectonically-controlled landforms.

Tectonism control is characterized by hot springs and waterfalls in the structure 1. Stage 1 analysis (drainage density + TWI), stage 2 analysis (drainage density + TWI + slope angle), and stage 3 analysis (drainage density + TWI + slope angle + lineament density) show 20 springs in potential landforms and 3 springs in less potential landforms (Figure 6). Structure 2 and structure 3 experience the addition of springs in the potential area after stage 3 analysis.

Table 3: Parameters of unconfined groundwater potential

Landforms	Study Parameters	Spring				Number of springs
		Potential	Area (km²)	Less Potential	Area (km²)	
Structure 1	drainage density + TWI	20	95.58	3	33.46	23
Structure 2		16	39.72	7	18.03	23
Structure 3		5	25.63	3	17.12	8
Total		41	160.93	13	68.61	54
Structure 1	drainage density + TWI + slope	20	91.82	3	37.06	23
Structure 2		16	37.45	7	20.36	23
Structure 3		5	26.48	3	16.37	8
Total		41	155.75	13	73.79	54
Structure 1	drainage density + TWI + slope + Lineamen Density	20	92.45	3	36.04	23
Structure 2		18	36.96	5	20.71	23
Structure 3		6	26.71	2	16.67	8
Total		44	156.12	10	73.42	54

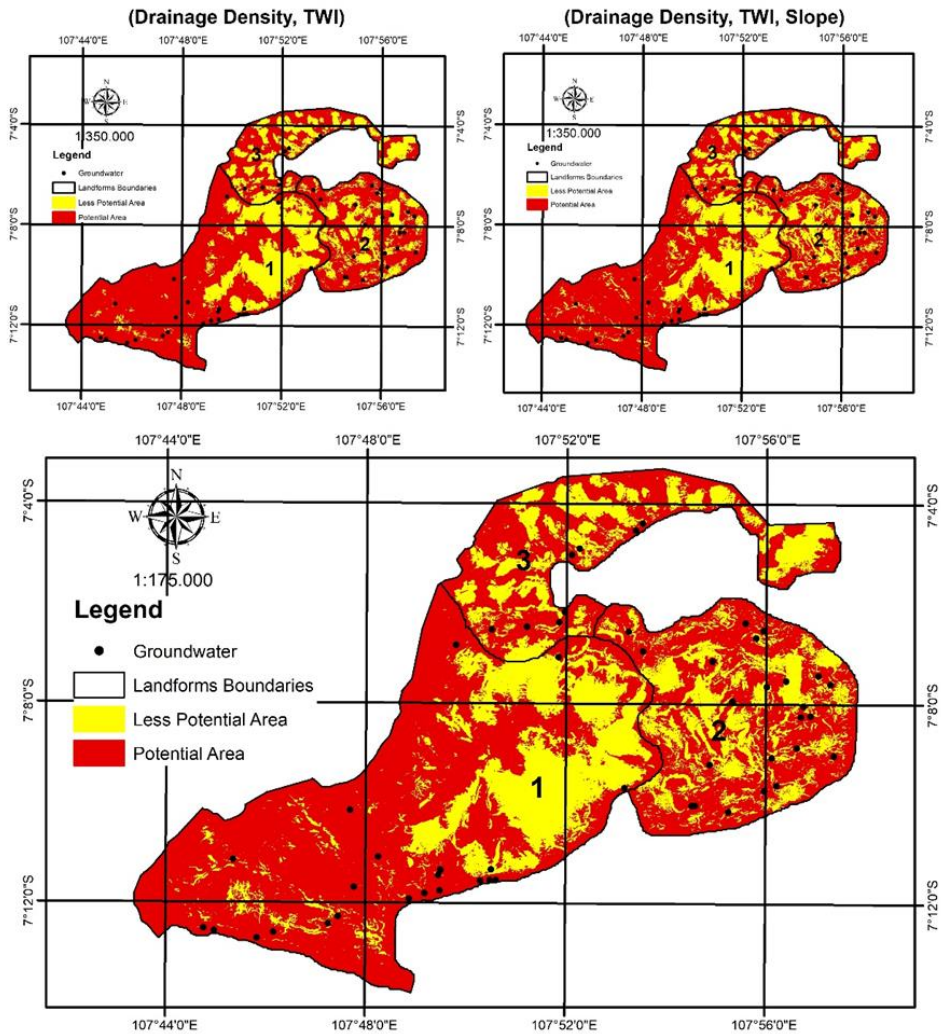


Figure 7: Distribution of unconfined groundwater potential zone

Analysis on stage 1 and 2 did not experience a change in the number of springs in the potential and less potential landforms (Table 2). Potential and less potential areas at each stage of analysis differ, due to the impact of the step-wise overlay results on raster data.

5. Conclusion

DEM-NAS is able to analyze the study of groundwater potential using parameters of drainage density, TWI (Topographic Wetness Index), slope angle and lineament density in tectonically-controlled landforms. Step wise overlay analysis shows that 44 springs are in the potential landforms with an area percentage (68.01%) and 10 springs are in less potential landforms with an area percentage (31.99%). The greatest value of the river flow density is located in the area of highland dominance but springs are rarely found, which is in structure 3. The condition of the relief unit and the process of landform formation affect the TWI value distribution. In general, the slope angle in the tectonically-controlled landforms is dominated by hilly to mountainous relief classes (16°-35°). The lineament density is determined by the number of lineaments and the area. The lineament of the extraction results using spatial technology is a valley or ridge in the tectonically-controlled landforms.

References

Al-adamat, R. and Al-shabeeb, A. A., 2017, A Simplified Method for the Assessment of Groundwater Vulnerability to Contamination. *Journal Water Resource and Protection*. Vol. 9, 305-321.

Al-rozouq, R., Shanableh, A., Merabtene, T., Siddique, M., Khalil, M. A., Idris, A. and Amulla, E., 2019, Potential Groundwater Zone Mapping Based on Geo-Hydrological Considerations and Multi-Criteria Spatial Analysis: North UAE. *Catena*, Vol. 173, 511-524.

Al-shabeeb, A. A., Al-adamat, R., Al-fugara, A. and Al-amoush, H., 2018, Groundwater for Sustainable Development Delineating Groundwater Potential Zones within the Azraq Basin of Central Jordan Using Multi-Criteria GIS analysis. *Groundwater for Sustainable Development*, Vol. 7, 82-90.

Andualem, T. G. and Demeke, G. G., 2019, Groundwater Potential Assessment Using GIS and Remote Sensing: A Case Study of Guna Tana Landscape, Upper blueNile Basin, Ethiopia. *Journal of Hydrology: Regional Studies*, Vol. 24, 100610.

Beven, K. J. and Kirkby, M. J., 1979, A Physically Based, Variable Contributing Area Model of Basin Hydrology. *Hydrological Sciences Bulletin*, Vol. 24, 43-69.

Das, S., 2019, Comparison among Influencing Factor, Frequency Ratio, and Analytical Hierarchy Process Techniques for Groundwater Potential Zonation in Vaitarna Basin, Mahasashtra, India. *Groundwater for Sustainable Development*, Vol. 8, 617-629.

Elbeih, S. F., 2015, An Overview of Integrated Remote Sensing and GIS for Groundwater Mapping in Egypt. *Ain Shams Engineering Journal*, Vol. 6, 1-15.

Gillin, C. P., Bailey, S. W., Mcguire, K. J. and Gannon, J. P., 2015, Mapping of Hydropedologic Spatial Patterns in a Steep Headwater Catchment. *Soil Science Society of America Journal*, Vol. 79, 440-453.

Grabs, T., Seibert, J., Bishop, K. and Laudon, H., 2009, Modeling Spatial Patterns of Saturated Areas: A Comparison of the Topographic Wetness Index and a Dynamic Distributed Model. *Journal of Hydrology*, Vol. 373(1-2), 15-23.

Hammouri, N. and Al-amoush, H., 2014, Groundwater Recharge Zones Mapping Using GIS: A Case Study in Southern Part of Jordan Valley, Jordan. *Arab J Geosci*, Vol. 7, 2815-2829.

Han, L., Liu, Z., Ning, Y. and Zhao, Z., 2018, Extraction and Analysis of Geological Lineaments Combining a DEM and Remote Sensing Images from the Northern Baoji Loess Area. *Advances in Space Research*, Vol. 62, 2480-2493.

Horton, R. E., 1932, Drainage Basin Characteristic. *Trans Am Geophys Union*, Vol. 13, 350-361.

Jenifer, M, A. and Jha, M. K., 2017, Comparison of Analytic Hierarchy Process, Catastrophe and Entropy Techniques for Evaluating Groundwater Prospect of Hard-Rock Aquifer Systems. *Journal of hydrology*, Vol. 548, 605-624.

Jha, M. K., Chowdary, V. M. and Chowdhury, A., 2010, Groundwater Assessment in Salboni Block, West Bengal (India) Using Remote Sensing, Geographical Information System and Multi-Criteria Decision Analysis Techniques. *Hydrogeol. J*. Vol. 18, 1713–1728.

Misi, A., Gumindoga, W. and Hoko, Z., 2018, An Assessment of Groundwater Potential and Vulnerability in the Upper Manyame Sub-Catchment of Zimbabwe. *Physics and Chemistry*

of the Earth, Vol. 105, 72-83.

Murmu, P., Kumar, M., Lal, D., Sonker, I. and Singh, S. K., 2019, Deleniation of Groundwater Potential Zones Using Geospatial Techniques and Analytichal Hierarchy Process in Dumka District, Jharkhand, India. *Groundwater Sustainable Development*, Vol. 9, 100239.

Murasingh, S., Jha, R. and Adamala, S., 2018, Geospatial Technique for Delineation of Groundwater Potential Zones in Mine and Dense Forest Area Using Weighted Index Overlay Technique. *Groundwater for Sustainable Development*, Vol. 7, 387-399.

Nejad, S. G., Falah, F., Daneshfar, M., Haghizadeh, A. and Rahmati, O., 2017, Deleniation of Groundwater Potential Zones Using Remote Sensing and GIS-based Data-Driven Models. *Geocarto International*, Vol. 32, 167-187.

Nithya, C. N., Srinivas, Y., Magesh, N. S. and Kaliraj, S., 2019, Assessment of Groundwater Potential Zones in Chittar basin, Southern India Using GIS Based AHP Technique. *Remote Sensing Applications: Society. Environment*, Vol. 15, 100248.

Oikonomidis, D., Dimogianni, S., Kazakis, N. and Voudouris, K., 2015, A GIS/Remote Sensing-based Methodology for Groundwater Potentiality Assessment in Tirnavos Area, Greece. *Journal of Hydrology*, Vol. 525, 197-208.

Patra, S., Mishra, P. and Chandra, S., 2018, Delineation of Groundwater Potential Zone for Sustainable Development: A Case Study from Ganga Alluvial Plain Covering Hooghly District of India Using Remote Sensing, Geographic Information System and Analytic Hierarchy Process. *Journal of Cleaner Production*, Vol. 172, 2485-2502.

Pham, B. T., Jaafari, A., Prakash, I., Singh, S. K., Quoc, N. K. and Bui, D. T., 2019, Hybrid Computational Intellegence Models for Groundwater Potential Mapping. *Catena*, Vol. 182, 104101.

Rajasekhar, M., Raju, G. S., Raju, R. S., Ramachandra, M. and Kumar, B. P., 2018, Data on Comparative Studies of Lineaments Extraction from Aster Dem, SRTM, And Cartosat for Jilledubanderu River Basin, Anantapur District, A.P, India by Using Remote Sensing and GIS. *Data in Brief*, Vol. 20, 1676-1682.

Razandi, Y., Pourghasemi, H. R., Neisani, N. S. and Rahmati, O., 2015, Application of Analytical Hierarchy Process, Frequency Ratio, and Certainty Factor Models for Groundwater Potential Mapping Using GIS. *Earth Sci. India*, Vol. 8, 867-883.

Sandoval, J. A. and Tiburan, C. L., 2019, Identification of Potential Artificial Groundwater Recharge Sites in Mount Makiling Forest Reserve, Philippines Using GIS and Analytical Hierarchy Process. *Applied Geography*, Vol. 105, 73-85.

Setiawan, O., Satohardi, J., Hadi, M. P. and Mardiatno, D., 2019, Delineating Spring Recharge Areas Infered from Morphological, Lithological, and Hydrological Datasets on Quaternary Volcanic Landscapes at the Southern Flank of Rinjani Volcano, Lombok Island, Indonesia. *Acta Geophysica*, Vol. 67, 177-190.

Singh, S. K., Zeddies, M., Shankar, U. and Grif, G. A., 2019, Potential Groundwater Recharge Zones within New Zealand. *Geoscience Frontier*, Vol. 10, 1065-1072.

Sorensen, R. and Seiber, J., 2007, Effects of DEM Resolution on the Calculation of Topographical Indices: TWI and its Components. *Journal of Hydrology*, Vol. 347, 79-89.

Thapa, R., Gupta, S., Guin, S. and Kaur, S., 2017, Assessment of Groundwater Potential Zones Using Multi-Influencing Factor (MIF) and GIS: A Case Study from Birbhum District, West Bengal. *Appl. Water Sci.*, Vol. 7, 4117-4131.

Tiede, D., 2014, A New Geospatial Overlay Method for the Analysis and Visualization of Spatial Change Patterns Using Object-Oriented Data Modeling Concepts. *Cartography Geographic Information Science*, Vol. 41, 227-234.

Van Zuidam, R. A., 1985, *Aerial Photo-Interpretation Terrain Analysis and Geomorphology Mapping*. (The Hague: SmithPublisher).

Venkateswaran, S. and Ayyandurai, R., 2015, Groundwater Potential Zoning in Upper Gadilam River Basin Tamil Nadu. *Aquatic Procedia*, Vol. 4, 1275-1282.

Wilson, J. P. and Gallant, J. C., 2000, *Digital Terrain Analysis*. (New York: Wiley Publisher).

Yeh, H. F., Cheng, Y. S., Lin, H. I. and Lee, C. H., 2016, Mapping Groundwater Recharge Potential Zone Using a GIS Approach in Hualian River, Taiwan. *Sustainable Environment Research*, Vol. 26, 33-43.

Yousif, M., Sabet, H. S., Ghoubachi, S. Y. and Aziz, A., 2018, Utilizing the Geological Data and Remote Sensing Applications for Investigation of Groundwater Occurrences, West El Minia, Western Desert of Egypt. *NRIAG Journal Astronomy Geophysics*, Vol. 7, 318-333